First-passage characteristics of biased diffusion in a planar wedge

Diandrew Lexter Dy* and Jose Perico Esguerra†
National Institute of Physics and University of the Philippines, Diliman, Quezon City, Philippines
(Received 23 September 2012; revised manuscript received 2 March 2013; published 17 July 2013)

We obtain compact, exact, analytical expressions for the first-passage-time distribution for a particle undergoing biased diffusion in a planar wedge for wedge angles π/p, where p is a positive integer. We then provide the long-time limit of the first-passage time and found it to be dependent on the drift direction and wedge angle. We finally provide exact expressions for the mean first-passage time for specific cases.

DOI: 10.1103/PhysRevE.88.012121 PACS number(s): 05.40.Jc, 02.50.Ga

I. INTRODUCTION

The biased diffusion model for stochastic processes in confined media has been widely studied in the literature because it can be applied to various physical phenomena. These applications include the voltage dependence of the current density due to the disorder in organic semiconductors [1], photoexcitation of carriers in a hydroxyl-terminated silicon surface [2], and spin transport in semiconductor heterostructures [3]. This was also used to calculate biomolecular diffusion rates [4] and model chemotaxis [5] as well as tissue growth [6].

The dynamics of the biased diffusion process is governed by the convection-diffusion equation:

$$\frac{\partial}{\partial t}\rho(\mathbf{r},t) = \nabla\cdot D(\mathbf{r})\nabla\rho(\mathbf{r},t) - \nabla\cdot\mathbf{v}(\mathbf{r})\rho(\mathbf{r},t), \qquad (1)$$

where $\rho(\mathbf{r},t)$ is the particle's probability density function (PDF), $D(\mathbf{r})$ is the diffusion coefficient, and $\mathbf{v}(\mathbf{r})$ is the drift. When the diffusing particle is unbounded, the analytical solution of Eq. (1) can be obtained for uniform and constant diffusion coefficient and drift [7]. When there are confining boundaries, the analytical solution for the PDF has been found only in a few cases and geometries. Previously solved exact models with absorbing boundaries include one-dimensional cases [7,8], where the prescription used was the image solution with varying weights. Series solutions for specific forms of the diffusion coefficient $Dr^{-\eta}$ and drift $(-kr + \kappa r^{-1-\eta})\hat{r}$ for $\eta \geqslant 0$ and for any wedge angle [9] have been found for absorbing boundaries. For constant diffusion coefficient and no drift, the solution was found exactly and in closed form when the wedge angle is π/p, where p is 2 or a positive odd integer [10]. Numerical methods have also been used [11]; however, issues such as numerical dispersion, instability, and accuracy of the solution in the boundary regions were encountered for bias-dominated processes.

Through the PDF, we can calculate the first-passage-time distribution (FPTD) of the particle. The FPTD describes the probability that a stochastic process reaches for the first time some specified values, e.g., boundaries. First-passage processes are encountered in the study of biological processes, particularly mechanochemical coupling in kinesins [12], in DNA translocation [13], in the translocation of polymers [14–16], and in the reaction rate for diffusion-controlled reactions [17]. However, only a limited number of exactly solvable models or geometries have been found for the FPTD, including one-dimensional cases [7,18] and planar wedge boundaries without drift [10]. For unbiased diffusion in arbitrary-angled planar wedge geometries, only the long-time limit has been solved [7,19]. Numerical procedures have also been implemented to solve for the FPTD when the drift is linear in space [20]. A closely related quantity to the FPTD is the survival probability; this has been studied for wedge systems [7,9,10,19,20].

In this paper, we solve the convection-diffusion Eq. (1) for absorbing planar-wedge geometries. We consider systems with constant and uniform diffusion coefficient and drift; this is applicable to incompressible velocity field in the context of the evolution of fluid vorticity for the Fokker-Planck equation [11,21] or for linear external field in the Smoluchowski equation [22]. We emphasize that this physical system is distinct from the system in Ref. [9], where the drift is radial. The two systems are equivalent only when there is no bias and the diffusion coefficient is uniform and constant in time. For specific angles, we provide exact closed-form expressions of the PDF (Sec. II), as well as the FPTD (Sec. III) to the boundary. We found that the long-time limit of the FPTD to be largely dependent on the wedge angle as well as the drift direction. We also provide exact expressions for the mean first-passage time (MFPT) (Sec. IV), or the average time that the particle reaches the boundary for the first time, for special cases of the drift direction and wedge angle.

II. PROBABILITY DENSITY FUNCTION

Our first task is to calculate the PDF of a diffusing particle with bias for the planar wedge boundary. We consider the particle initially at (x_0, y_0) constrained in a wedge such that the absorbing boundaries are at $y = \pm x\tan\beta$, where 2β is the angle of the wedge. The PDF is the solution to the convection-diffusion Eq. (1), with initial condition $\rho(x,y;t=0) = \delta(x-x_0)\delta(y-y_0)$, and absorbing boundary condition $\rho(x,y,t)|_{y=\pm x\tan\beta} = 0$. To solve this partial differential equation, we recall the Green's function for the unbounded convection-diffusion equation with Dirac δ initial condition is

$$G(x_0,y_0;t) = \frac{1}{4\pi Dt} e^{-\frac{(x-x_0-v_x t)^2}{4Dt}} e^{-\frac{(y-y_0-v_y t)^2}{4Dt}}. \qquad (2)$$

To satisfy the boundary conditions, a superposition of expressions of this type is needed. We employ the method of images to find this combination. The wedge system, for example, can

*ddy@nip.upd.edu.ph
†jesguerra@nip.upd.edu.ph

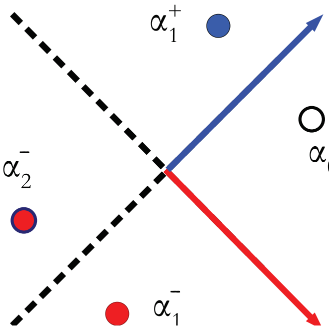

FIG. 1. (Color online) Particle initially located at α_0 inside a wedge with boundaries at $y = \pm x \tan\beta$ for wedge angle $2\beta = \pi/4$. The images located at α_n^+ and α_n^- are also indicated.

be thought of as two half planes separated by an angle. We first comment on the half-plane image solution in the context of convection-diffusion equation.

For the half plane $x > 0$, the solution is just the superposition

$$\rho = G(x_0, y_0) - AG(-x_0, y_0), \tag{3}$$

where $-A = -e^{-v_x x_0/D}$ is the weight of the image needed to satisfy the absorbing conditions. This result is an extension of the one-dimensional case found in Ref. [7]. We now generalize this result to the planar boundary defined by $y = x \tan\beta$. For a particle initially at $(r\cos\alpha, r\sin\alpha)$, such that $\alpha < \beta$, the reflected image can be seen to be at the angle $2\beta - \alpha$. We find that

$$\rho = G(\mathbf{r}_0) - A(\alpha)G(\mathbf{r}_1), \tag{4}$$

where $\mathbf{r}_1$ is the image position, (v,θ) are, respectively, the magnitude and polar angle of the drift, and $A(\alpha,\beta) = e^{-\frac{rv}{D}\sin(\beta-\theta)\sin(\beta-\alpha)}$. We note here that this superposition does not work for spatially dependent diffusion coefficient and drift.

We can now calculate the PDF for absorbing wedge boundary defined by $y = \pm x \tan\beta$. Let the particle be initially at $(x_0, y_0) = (r\cos\alpha_0, r\sin\alpha_0)$ as shown in Fig 1. The image of the particle on the upper boundary, $y = +x\tan\beta$, is at a radius r and an angle $\alpha_1^+ = 2\beta - \alpha_0$. The reflection on the lower boundary, $y = -x\tan\beta$, is at $\alpha_1^- = -(2\beta + \alpha_0)$. We now reflect the image at α_1^+ on the lower boundary, which we find at an angle $\alpha_2^+ = -(4\beta - \alpha_0)$. The reflection of the image at α_1^- on the upper boundary yields the angle at $\alpha_2^- = 4\beta + \alpha_0$. For n reflections, with the images getting reflected alternately with the upper and lower boundaries, we get the angles

$$\alpha_n^+ = (-1)^{n-1}(2n\beta - \alpha_0) \quad \alpha_n^- = (-1)^n(2n\beta + \alpha_0), \tag{5}$$

and at the same distance from the origin, r. The superscript in our notation here denotes whether the first reflection is at the upper $(+)$ or the lower $(-)$ boundary. We impose that the wedge angles be $2\beta = \pi/p$, where p is a positive integer, which implies that the last reflection from both the upper and lower boundaries coincide. For these wedge angles, and repeated reflection of the images for two half planes, the PDF of our system is

$$\rho = G(\alpha_0) + (-1)^p \prod_{m=1}^{p} A_m(\alpha_m^+,\beta)G(\alpha_p) + \sum_{n=1}^{p-1}(-1)^n \prod_{m=1}^{n}\left[A_m(\alpha_m^+,\beta)G(\alpha_n^+) + A_m(\alpha_m^-,-\beta)G(\alpha_n^-)\right], \tag{6}$$

where

$$A_m(\alpha,\beta) = e^{-\frac{rv}{D}\sin((-1)^m\beta-\theta)\sin((-1)^m\beta-\alpha)}. \tag{7}$$

This solution is valid only within the wedge, $(-\beta,\beta)$, and is zero outside of the wedge.

III. FIRST-PASSAGE-TIME DISTRIBUTION

The first-passage-time distribution to the boundary can now be calculated for our wedge system through the formula

$$F(t) = -\frac{d}{dt}\int \rho(\mathbf{r},t)d\sigma, \tag{8}$$

where the integral is an area integral over the wedge. Evaluation of this integral is not straightforward, but for unbiased diffusion it has been done for specific wedge angles π/p, where p is 2 or an odd integer [10]. For other cases, however, it is not straightforward to evaluate this integral. Instead of directly evaluating the integral in Eq. (8), we first express the FPTD as

$$F(t) = -\int d\sigma(D\nabla\cdot\nabla\rho - \mathbf{v}\cdot\nabla\rho). \tag{9}$$

For constant $\mathbf{v}$, the above expression reduces to

$$F(t) = \int (D\nabla\rho - \mathbf{v}\rho)\cdot d\hat{n}, \tag{10}$$

where the line integral is over the wedge boundaries and $\hat{n}$ is the inward unit vector normal to the boundary. Because of absorbing boundary conditions, the second-term integral vanishes. Thus, the FPTD is equal to the flux of the PDF at the wedge boundaries.

In general, the contributions to the integral of the upper boundary and the lower boundary are not equal and are dependent on the initial position of the particle as well as the drift velocity. Evaluation of the line integral over the upper boundary is easier if we rotate our coordinate axis through the rotation matrix:

$$\begin{pmatrix}\bar{x}_1\\ \bar{y}_1\end{pmatrix} = \begin{pmatrix}\cos\beta & \sin\beta\\ -\sin\beta & \cos\beta\end{pmatrix}\begin{pmatrix}x\\ y\end{pmatrix}. \tag{11}$$

Here, the upper boundary is rotated clockwise such that it is now a line $\bar{y}_1 = 0$ and $\hat{n}_{\rm ub} = -\hat{\bar{y}}$. Similarly, the integral over the lower boundary can be evaluated by rotating our axis counter-clockwise by β, such that the lower boundary line is at $\bar{y}_2 = 0$ and that $\hat{n}_{\rm lb} = \hat{\bar{y}}_2$. The FPTD is then determined by adding these two line integral contributions:

$$F(t) = \int_0^\infty \left.\frac{\partial\rho}{\partial\bar{y}_2}\right|_{\bar{y}_2=0} d\bar{x}_2 - \int_0^\infty \left.\frac{\partial\rho}{\partial\bar{y}_1}\right|_{\bar{y}_1=0} d\bar{x}_1. \tag{12}$$

To make our expressions for the FPTD concise, we first define the line integral for the unbounded solution $G(\alpha)$ over the lower boundary:

$$\begin{aligned} f(\alpha,\beta) &= \int_0^\infty \left.\frac{\partial G(\alpha)}{\partial \bar{y}}\right|_{\bar{y}_2=0} d\bar{x}_2 \\ &= \frac{r\sin(\beta+\alpha)+vt\sin(\beta+\theta)}{8\sqrt{Dt^3\pi}} \\ &\quad\times \exp\left\{\frac{-[r\sin(\alpha+\beta)+vt\sin(\beta+\theta)]^2}{4Dt}\right\} \\ &\quad\times \left\{1+\operatorname{erf}\left[\frac{r\cos(\beta+\alpha)+vt\cos(\beta+\theta)}{\sqrt{4Dt}}\right]\right\}. \end{aligned} \tag{13}$$

The line integral over the whole wedge boundary for the unbounded Green's function solution is, thus, defined as

$$\begin{aligned} g(\alpha) &= \int_0^\infty \left.\frac{\partial G}{\partial \bar{y}_2}\right|_{\bar{y}_2=0} d\bar{x}_2 - \int_0^\infty \left.\frac{\partial G}{\partial \bar{y}_1}\right|_{\bar{y}_1=0} d\bar{x}_1 \\ &= f(\alpha,\beta) - f(\alpha,-\beta), \end{aligned} \tag{14}$$

where the last line is due to symmetry. We can now express the FPTD as

$$\begin{aligned} F(t) &= g(\alpha_0) + (-1)^p g(\alpha_p^+) \prod_{m=1}^{p} A_m(\alpha_{m-1}^+,\beta) \\ &\quad + \sum_{n=1}^{p-1}(-1)^n \left[g(\alpha_n^+) \prod_{m=1}^{n} A_m(\alpha_{m-1}^+,\beta) \right. \\ &\quad \left. + g(\alpha_n^-) \prod_{m=1}^{n} A_m(\alpha_{m-1}^-,-\beta) \right], \end{aligned} \tag{15}$$

where $\alpha_n^+ = (-1)^{n-1}(2n\beta - \alpha)$, $\alpha_n^- = (-1)^n(2n\beta+\alpha)$, and $A_m(\alpha,\beta) = e^{\frac{-rv}{D}\sin[(-1)^m\beta-\theta]\sin[(-1)^m\beta-\alpha]}$. This expression for the FPTD is the main result of this paper and is valid for any wedge of angle π/p, where p is a positive integer. To illustrate this result, we plot the FPTD for a specific case, where the wedge angle is $\pi/4$ and the drift velocity is along the x direction. The plot is shown in Fig. 2.

The long-time limit of the FPTD for the biased case ($v \neq 0$) simplifies to

$$F(\alpha_0)_{\substack{t\to\infty \\ v\neq 0}} = \begin{cases} C\frac{v\sin(\beta+\theta)}{4\sqrt{Dt\pi}} e^{-v^2t\sin^2(\beta+\theta)/4D} + C\frac{v\sin(\beta-\theta)}{4\sqrt{Dt\pi}} e^{-v^2t\sin^2(\beta-\theta)/4D}; & \beta-\frac{\pi}{2} \leqslant \theta \leqslant \frac{\pi}{2}-\beta \\ C\frac{v\sin(\beta+\theta)}{4\sqrt{Dt\pi}} e^{-v^2t\sin^2(\beta+\theta)/4D}; & -\beta-\frac{\pi}{2} \leqslant \theta < \beta-\frac{\pi}{2} \\ C\frac{v\sin(\beta-\theta)}{4\sqrt{Dt\pi}} e^{-v^2t\sin^2(\beta-\theta)/4D}; & -\beta+\frac{\pi}{2} \leqslant \theta < \beta+\frac{\pi}{2} \\ C\frac{[\tan(\beta+\theta)+\tan(\beta-\theta)]}{4t\sqrt{\pi}} e^{-v^2t/4D}; & |\theta| > \beta+\frac{\pi}{2} \end{cases}, \tag{16}$$

where the constant C is

$$\begin{aligned} C &= 1 + (-1)^p + \prod_{m=1}^{p} A_m(\alpha_{m-1}^+,\beta) \\ &\quad + \sum_{n=1}^{p-1}(-1)^n\left[\prod_{m=1}^{n} A_m(\alpha_{m-1}^+,\beta) + \prod_{m=1}^{n} A_m(\alpha_{m-1}^-,-\beta)\right]. \end{aligned} \tag{17}$$

For the unbiased case, the FPTD falls with $t^{-3/2}$, as previously derived in Refs. [7,10]. In the presence of the drift, however, we observe an exponential time decay factor for the long-time limit, suggesting that the FPTD falls faster in the presence of a drift. We can characterize the FPTD for the biased case, depending on the scale factor $t^{-1/2}$ or t^{-1} and on the direction of the drift. When $|\theta| > \beta + \frac{\pi}{2}$, the FPTD falls fastest, which we characterize as the particle going effectively toward the boundary. When $\beta - \frac{\pi}{2} < \theta < \frac{\pi}{2} - \beta$, the FPTD falls slowest, which characterizes to the particle effectively moving away from the boundary.

IV. MEAN FIRST-PASSAGE-TIME

The standard MFPT formula [7],

$$\langle t \rangle = \int_0^\infty tF(t)dt, \tag{18}$$

gives a meaningful average value when the survival probability $S(t) = \int \rho d\sigma = 1 - \int_0^t F(t')dt'$ approaches zero at long times, i.e., all particles will eventually reach the boundary. In the presence of the drift, however, the survival probability does not vanish at long times. Explicitly calculating the survival

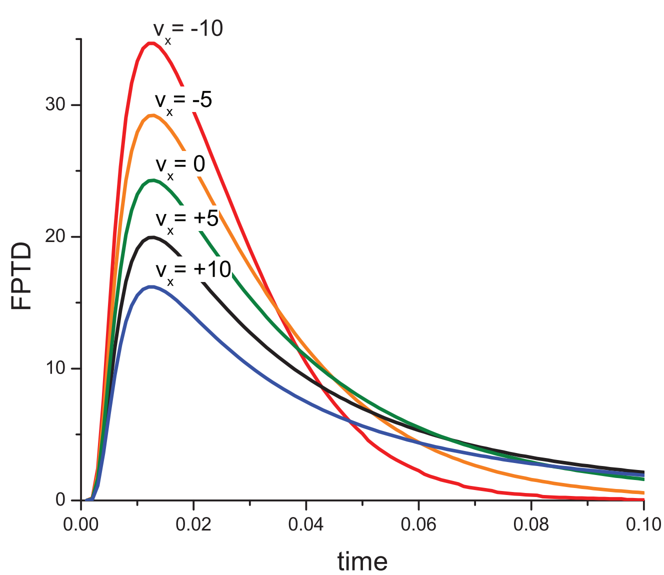

FIG. 2. (Color online) FPTD of a particle initially at $\alpha_0 = 0$ inside a wedge of angle $\pi/4$. The drift velocity here is set in the x direction. We set the parameters $D = 1/2$ and $r = 1$.

probability in the long-time limit using our expression for the PDF (6), we obtain

$$S(t)|_{t\to\infty} = C\mathrm{erf}\left(\frac{v\sqrt{t}\sin(\beta+\theta)}{2\sqrt{D}}\right) - C\mathrm{erf}\left(\frac{v\sqrt{t}\sin(\beta-\theta)}{2\sqrt{D}}\right), \tag{19}$$

where the constant C is written in Eq. (17). The long-time limit of the survival probability does not vanish when $-\beta \leqslant \theta \leqslant \beta$ and $v \neq 0$. For this case, we define the normalized mean first-passage time (NMFPT) as

$$\langle \tilde{t} \rangle = \int_0^\infty t\tilde{F}(t)dt, \tag{20}$$

where $\tilde{F}(t) = F(t)/(\int_0^\infty F(t')dt')$ is the normalized FPTD. For other cases, the FPTD is already normalized and reproduces the standard definition of the NMFPT [7].

For the unbiased diffusion, the NMFPT have been solved for any wedge angle [7]. For $\mathbf{v} \neq 0$, however, this solution is not as straightforward. In this work, we use the exact FPTD expressions to derive the mean time through the integral Eq. (20). For some special cases, exact evaluation of this integral is possible.

A. Unbiased diffusion on a wedge

For the unbiased diffusion ($\mathbf{v} = 0$), we have $A = 1$ regardless of the placement of the image. The FPTD, thus, simplifies to

$$F(\alpha_0)_{p,\mathrm{even}} = \frac{1}{2\sqrt{Dt^3\pi}} \sum_{n=1}^{p} (-1)^{n-1} r\sin[(2n-1)\beta+\alpha_0] \times e^{\frac{-r^2\sin^2([2n-1]\beta+\alpha_0)}{4Dt}} \mathrm{erf}\left\{\frac{r\cos[(2n-1)\beta+\alpha_0]}{\sqrt{4Dt}}\right\}$$

$$F(\alpha_0)_{p,\mathrm{odd}} = \frac{1}{2\sqrt{Dt^3\pi}} \sum_{n=1}^{p} (-1)^{n-1} r\sin[(2n-1)\beta+\alpha_0] \times e^{\frac{-r^2\sin^2[(2n-1)\beta+\alpha_0]}{4Dt}}. \tag{21}$$

This result is applicable for any wedge of angle $2\beta = \pi/p$, where p is a positive integer. The FPTD here is normalized since for the unbiased case, the survival probability (19) vanishes at long times. This is a generalization of the result in Ref. [10], where the closed form expression is determined only when p is 2 or an odd integer. The vanishing long-time limit of the survival probability implies that this FPTD is normalized. We now calculate the mean first-passage-time for this distribution for each case where p is even or odd.

The MFPT can be calculated as

$$\bar{t}_{p\neq 2,\mathrm{even}} = \frac{r^2}{2D} \sum_{n=1}^{p} \frac{(-1)^{n-1}\sin[(2n-1)2\beta+2\alpha_0]}{\pi} \times \left\{1-\tan[(2n-1)\beta+\alpha_0] \times \left[\frac{\pi}{2}-(2n-1)\beta-\alpha_0\right]\right\}$$

$$\bar{t}_{p\neq 1,\mathrm{odd}} = \frac{r^2}{2D} \sum_{n=1}^{p} (-1)^n \sin^2[(2n-1)\beta+\alpha_0], \tag{22}$$

and it diverges for $p = 1,2$. The exact expression of the MFPT here agrees with that of the results derived in Ref. [7] by a different approach.

B. Biased diffusion on a half-plane

We now consider some special cases for the biased diffusion. We first consider the biased diffusion on a half-plane, or when $\beta = \pi/2$. For this case, the FPTD simplifies to

$$F(t)_{p=1} = \frac{r\cos\alpha_0}{2\sqrt{Dt^3\pi}} \exp\left[-\frac{(r\cos\alpha_0 + vt\cos\theta)^2}{4Dt}\right], \tag{23}$$

which is consistent with that found in Ref. [7]. The normalized FPTD can be computed to $\tilde{F}(t) = F(t)/N$, where $N = e^{-\frac{rv\cos\alpha(\cos\theta+|\cos\theta|)}{2D}}$. The MFPT and NMFPT can then be calculated to

$$\langle \tilde{t} \rangle_{p=1} = \frac{\langle t \rangle_{p=1}}{N} = \frac{r\cos\alpha_0}{v|\cos\theta|}. \tag{24}$$

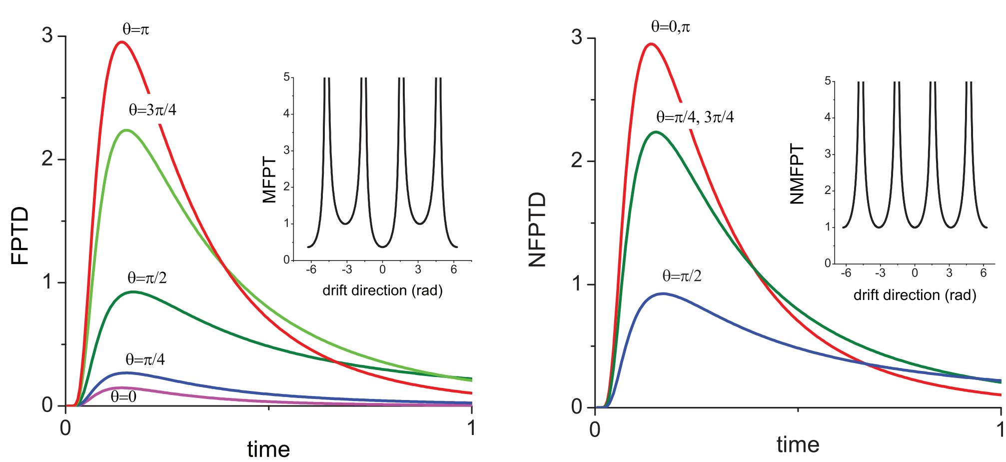

FIG. 3. (Color online) FPTD and the NFPTD with their corresponding MFPT and NMFPT (inset) of the biased diffusion in the half-plane for several drift direction θ. We set the parameters $\alpha_0 = 0, v = 2, r = 1$ and $D = 1$.

The effect of the drift direction to the half-plane for the FPTD, NFPTD, MFPT, and NMFPT is illustrated in Fig. 3. The NFPTD when the drift direction θ goes away from the boundary is equal to the FPTD for drift direction $\pi - \theta$. In the limit where $v \to 0$, the MFPT and NMFPT diverges, which is consistent with the results for the unbounded diffusion. We see that the presence of a nonzero drift for this case causes the MFPT and NMFPT to be finite except when the drift direction is at $\theta = \pm\frac{\pi}{2}$.

C. Vertical bias in a π/p-wedge with $p > 1$ and odd

We now consider the case where the drift direction is vertical and for special wedge angles π/p, where p is odd and $p > 1$. The FPTD here is normalized from the long-time limit of the survival probability, Eq. (19). We can evaluate the MFPT exactly for this case as

$$\langle t_\pm\rangle = \langle \tilde{t}_\pm\rangle = j_{t\pm}(\alpha_0) + (-1)^p j_{t\pm}(\alpha_p^+)\prod_{m=1}^{p} A_m(\alpha_{m-1}^+,\beta) + \sum_{n=1}^{p-1}(-1)^n j_{t\pm}(\alpha_n^+)\left[\prod_{m=1}^{n} A_m(\alpha_{m-1}^+,\beta) + j_{t\pm}(\alpha_n^-)\prod_{m=1}^{n} A_m(\alpha_{m-1}^-,-\beta)\right], \tag{25}$$

where we define the functions

$$j_{t\pm}(\alpha) = \frac{e^{\frac{-rv}{2D}\cos\beta[\pm\sin(\alpha+\beta)+|\sin(\alpha+\beta)|]}}{4v^2\cos^2(\beta)} \times \{rv\cos(\beta)[\pm\sin(\alpha+\beta)+|\sin(\alpha+\beta)|]\pm 2D\} + \frac{e^{\frac{-rv}{2D}\cos\beta[\pm\sin(\alpha-\beta)+|\sin(\alpha-\beta)|]}}{4v^2\cos^2(\beta)} \times \{rv\cos(\beta)[\pm\sin(\alpha-\beta)+|\sin(\alpha-\beta)|]\pm 2D\}. \tag{26}$$

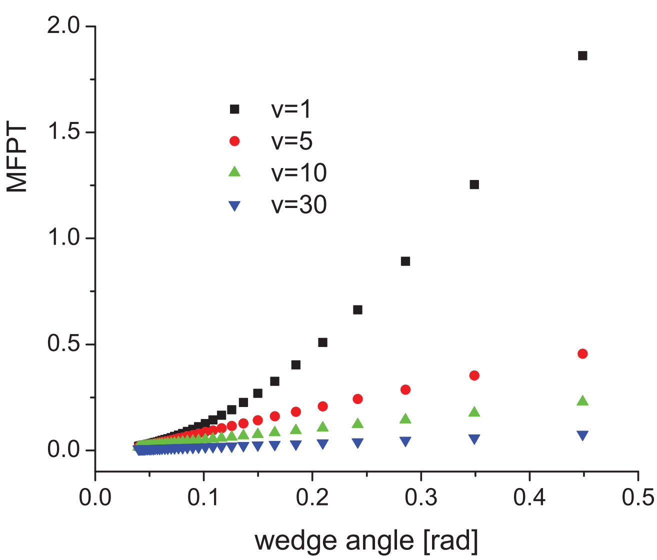

FIG. 4. (Color online) MFPT of the particle initially at the middle ($\alpha_0 = 0$) for several wedge angles $2\beta = \pi/p$ and drift speed. We set the parameters $D = 1$ and $r = 10$.

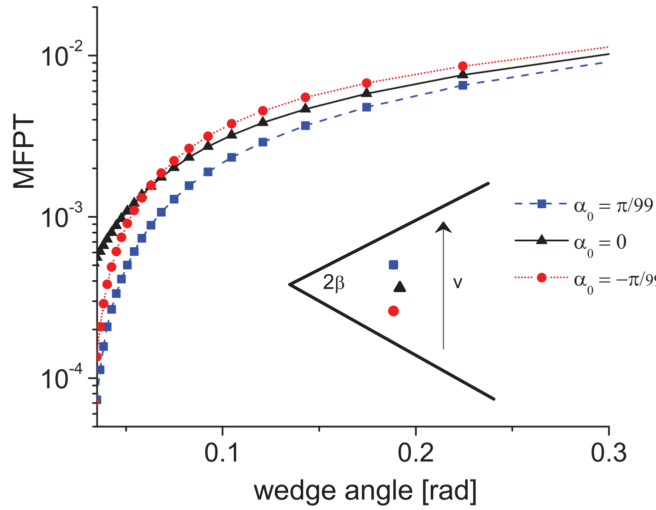

FIG. 5. (Color online) MFPT of the particle with upward bias for several wedge angles $2\beta = \pi/p$, with p an odd integer. The initial position of the particle is set at $\alpha_0 = \pi/99, 0, -\pi/99$ (see inset). We set the parameters $D = r = 1$ and $v = 30$. The data points here are exact.

In our notation, the subscripts + and − refer to the drift directions $\theta = \pi/2$ and $\theta = -\pi/2$, respectively. We see here that the MFPT is equal for both bias directions. We plot the MFPT for several angles and drift speed in Fig. 4. We observe that for small wedge angles, the MFPT goes to zero.

An interesting property of the MFPT for the vertical bias case is that it does not vary monotonically with the distance of the particle's initial position to the boundary. To illustrate this behavior, we plot the MFPT for several wedge angles in Fig. 5, when the particle is initially at $\alpha_0 = \pi/99$, $\alpha = 0$, and $\alpha = -\pi/99$. We see that the MFPT for the three cases increase as the wedge angle is increased. However, the order of the values of the MFPT for these three cases changes as we increase the wedge angle. For small wedge angles, we see that $\langle t\rangle_{\alpha=+\pi/99} < \langle t\rangle_{\alpha=-\pi/99} < \langle t\rangle_{\alpha=0}$. For large angles, however, this order changes to $\langle t\rangle_{\alpha=+\pi/99} < \langle t\rangle_{\alpha=0} < \langle t\rangle_{\alpha=-\pi/99}$. We also observe that at large angles, the MFPT for each case becomes closer to each other. This is a consequence of the distance of the initial position to the boundary being close to equal for the three cases.

V. CONCLUSION

In this paper, we studied the biased diffusion in a planar wedge for wedge angles π/p, where p is a positive integer. We obtained compact, exact, analytical expressions for the first-passage-time distribution for this system and provided conditions for the wedge angle and drift direction, wherein the particle effectively moves away and toward the boundary. We finally provided exact expressions for the mean first-passage time for specific cases of the bias and wedge angle and found that it does not vary monotonically with the distance of the particle's initial position to the boundary.

[1] S. L. M. van Mensfoort and R. Coehoorn, Phys. Rev. B **78**, 085207 (2008).
[2] R. A. Murdick, R. K. Raman, Y. Murooka, and C. Y. Ruan, Phys. Rev. B **77**, 245329 (2008).
[3] M. K. Chan, Q. O. Hu, J. Zhang, T. Kondo, C. J. Palmstrom, and P. A. Crowell, Phys. Rev. B **80**, 161206 (2009).
[4] G. Zou, R. Skeel, and S. Subramaniam, Biophys. J. **79**, 638 (2000).
[5] E. Keller and L. Segel, J. Theor. Biol. **30**, 225 (1971).
[6] G. Cheng, P. Markenscoff, and K. Zygourakis, Biophys. J. **97**, 401 (2009).
[7] S. Redner, *A Guide to First-Passage Processes* (Cambridge University Press, Cambridge, 2001).
[8] A. Molini, P. Talkner, G. Katul, and A. Porporato, Physica A **390**, 1841 (2011).
[9] E. K. Lenzi, L. R. Evangelista, M. K. Lenzi, and L. R. da Silva, Phys. Rev. E **80**, 021131 (2009).
[10] Diandrew Lexter Dy and J. P. Esguerra, Phys. Rev. E **78**, 062101 (2008).
[11] P. Szymczak and A. J. C. Ladd, Phys. Rev. E **68**, 036704 (2003).
[12] A. B. Kolomeisky, E. B. Stukalin, and A. A. Popov, Phys. Rev. E **71**, 031902 (2005).
[13] R. C. Lua and A. Y. Grosberg, Phys. Rev. E **72**, 061918 (2005).
[14] J. K. Wolterink, G. T. Barkema, and D. Panja, Phys. Rev. Lett. **96**, 208301 (2006).
[15] A. Gopinathan and Y. W. Kim, Phys. Rev. Lett. **99**, 228106 (2007).
[16] J. L. A. Dubbeldam, A. Milchev, V. G. Rostiashvili, and T. A. Vilgis, Phys. Rev. E **76**, 010801 (2007).
[17] A. Szabo, K. Schulten, and Z. Schulten, J. Chem. Phys. **72**, 4350 (1980).
[18] S. B. Yuste and K. Lindenberg, Phys. Rev. E **69**, 033101 (2004).
[19] S. Redner and P. L. Krapivsky, Am. J. Phys. **67**, 1277 (1999).
[20] Z. Hu, L. Cheng, and B. Berne, J. Chem. Phys. **133**, 034105 (2010).
[21] R. B. Bird, W. E. Stewart, and E. N. Lightfoot, *Transport Phenomena* (Wiley, New York, 1960).
[22] H. Risken, *The Fokker-Planck Equation: Methods of Solution and Applications* (Springer, Berlin, 1996).